

Melanite-bearing nepheline syenite fragments and $^{40}\text{Ar}/^{39}\text{Ar}$ age of phlogopite megacrysts in conduit breccia from the Poços de Caldas Alkaline Massif (MG/SP), and implications

Silvio Roberto Farias Vlach^{1*}, Horstpeter Herberto Gustavo Jose Ulbrich¹, Mabel Norma Costas Ulbrich¹, Paulo Marcos Vasconcelos²

ABSTRACT: The Poços de Caldas Alkaline Massif, located in southeast Brazil, is composed of tinguaites, as well as phonolites and nepheline syenites (NeS), together with assorted pyroclastic rocks. The latter constitute deposits within the Vale do Quartel, and show fragments of alkaline rocks (NeS, tinguaites), basaltic and ultramafic volcanics/subvolcanics, sandstones, and quartz-feldspathic rocks from the crystalline basement. NeS fragments with melanite, previously unknown, and cm-sized fragments of phlogopite megacrysts from related conduit breccia were chosen for detailed studies. The NeS fragments are medium- to coarse grained and contain K-feldspar (Or_{95-83}), secondary albite (Ab_{99}), altered nepheline, clinopyroxene (diopside, minor hedenbergite) and partially altered, zoned, idiomorphic melanite. These NeS fragments are typically metaluminous, and point to the existence of similar intrusions hidden at depth, an important input to the massif's petrology. The phlogopite megacrysts are compositionally homogeneous, with high Ti, Mg and Al contents; Ba and F are minor components. Two phlogopite aliquots were dated and yielded identical $^{40}\text{Ar}/^{39}\text{Ar}$ plateau ages of $87.1(\pm 0.5)$ Ma and $86.6(\pm 0.5)$ Ma, which represent minimum and maximum values for phlogopite crystallization and breccia emplacement, respectively. Previously obtained ages for the Poços de Caldas rocks are concentrated in the 75–86 Ma range interval.

KEYWORDS: Melanite-bearing nepheline syenite fragments; phlogopite megacrysts; conduit breccia; $^{40}\text{Ar}/^{39}\text{Ar}$ age; Poços de Caldas Alkaline Massif.

INTRODUCTION

The Poços de Caldas alkaline massif is one of the largest intrusions of its kind (around 800 km²), comparable in size to the kindred Lovozero (Kola Peninsula, 600 km²) and the Pilansberg (South Africa) intrusions, and second only to the Khibina massif, Kola Peninsula (1,350 km²). It is one of over a hundred alkaline occurrences that cut across the so-called Brazilian Platform, a manifestation of orogenic revival (the “Wealdenian reactivation”; Almeida 1983) that mainly emplaces alkaline intrusions along the northern and eastern margins of the large volcano-sedimentary Paraná Basin. The massif itself is the westernmost occurrence of a series of intrusions that form an arc-like structure, the “Poços de Caldas-Cabo Frio seismo-tectonic lineament” (Sadowski

& Dias Neto 1981), which continues to the east with the sequentially younger Passa Quatro and Itatiaia, Barra do Pirai, Morro Redondo, Canaã, Tinguá, Rio Bonito, Morro de São João and, finally, the Cabo Frio occurrences. This belt was interpreted to be the result of sublithospheric mantle-plume activity, which pierced the continental lithosphere at intervals that are roughly consistent with assumed plate-displacement speeds (e.g. Sadowski & Dias Neto 1981, Ulbrich & Gomes 1981, Comin-Chiaramonti & Gomes 2005).

This study focuses on better defining the petrography of conduit breccias that appear sporadically in the Poços de Caldas massif. Conduit breccia, a material usually neglected in petrology, may sample unexposed rock types and helps to understand some aspects of the magmatic evolution of the massif. We present petrographic and

¹Department of Mineralogy and Geotectonics, Institute of Geoscience, São Paulo University – São Paulo (SP), Brazil. E-mails: srfvlach@usp.br, hulbrich@usp.br, mulbrich@usp.br

²School of Earth Sciences, University of Queensland – Queensland, Australia. E-mail: p.vasconcelos@uq.edu.au

*Corresponding author.

Manuscript ID 20170095. Received on: 07/10/2017. Approved on: 03/03/2018.

mineralogic characterizations of previously unknown melanite (Ti-andradite) -bearing nepheline syenite fragments, as well as of phlogopite megacrysts, common mineral fragments found in the breccia. $^{40}\text{Ar}/^{39}\text{Ar}$ ages for selected phlogopite macrocrysts are reported, adding important data to an age framework currently being refined.

GEOLOGIC BACKGROUND

The Poços de Caldas alkaline massif (Fig. 1) shows a roughly subcircular outline, with some smaller, bulge-like irregularities found especially along its northern site (location of the main lujavrite-khibinite occurrence) and its south-western part (the “Águas da Prata structure”; Ulbrich 1984). Most of its perimeter is marked by a well-developed topographic outline, especially pronounced along its northern

and southern limits, constituting “topographic rims”, which in the earlier literature were taken as the topographic expression of ring-dikes, fitting a “caldeira model” of emplacement (Ellert 1959). However, they are most likely the result of differential erosion (massive tinguaites are more resistant than syenites, which concentrate in the interior of the massif).

The district was mapped for the first time by R. Ellert, J.M.V. Coutinho and A.J.S. Björnberg (Ellert 1959, Björnberg 1959). Later mapping work was done by Bushee (1971) and geologists from the Nuclebrás state enterprise. The latter present a new map emphasizing hydrothermally altered areas and related mineralizations, such as caldasite (a zircon-baddeleyite intergrowth) and zircon occurrences, and breccia-hosted U deposits. H. Ulbrich mapped the main nepheline syenites (NeS) and the lujavrite-khibinite intrusions in detail (Ulbrich 1984, Ulbrich & Ulbrich 2000, Ulbrich *et al.* 2005; *cf.* also Schorscher & Shea 1992; Fig. 1).

The intrusion is made up of massive, mostly aphyric, tinguaites (subvolcanic intrusive phonolites), together with minor amounts of phonolites and many different types of NeS. The fine-grained rocks occupy around 70% of the district, and the NeS, no more than 20%. The NeS (mostly medium- to coarse-grained rocks) are clearly intrusive into the fine-grained varieties, thus leading to an unusual geologic pattern, as pointed out by the title of a pioneering reference that studied the district: the “coexistence of plutonic and volcanic rocks”, by Derby (1887). These rocks are made up mainly of K-feldspar, nepheline, sodic-calcic and sodic pyroxenes as main rock-forming phases; a few NeS present biotite (Ulbrich 1983, 1993).

The NeS can be divided, on the basis of mineralogical and geochemical features, into agpaite (typical peralkaline), largely subordinate, and predominant intermediate-miaskitic (slightly metaluminous to slightly peralkaline) varieties (*cf.* definitions in Sorensen 1974a). The first ones are recognized in Poços de Caldas by the presence of pink eudyalite, joined by several rare-metal silicates (*e.g.*, astrophyllite, lamprophyllite, rinkite), a useful criterion to separate agpaites from miaskites and intermediate rocks in the field. Eudyalite, in fact, can become a rock-forming mineral in lujavrites (meso- to melanocratic, foliated, eudyalite NeS, rich in incompatible elements) and khibinites (leucocratic massive eudyalite NeS, with analogous geochemical patterns; *cf.* Sorensen 1974b). A similar subdivision applies to tinguaites and phonolites, although they do not contain significant amounts of eudyalite and the diagnosis depends, in general, on thin section analysis under the microscope (*e.g.*, Ulbrich 1983, 1993).

Hydrothermal alteration, frequently associated with mineralizations, may affect all rock types in varying proportions. It is fairly concentrated in “circular structures”,

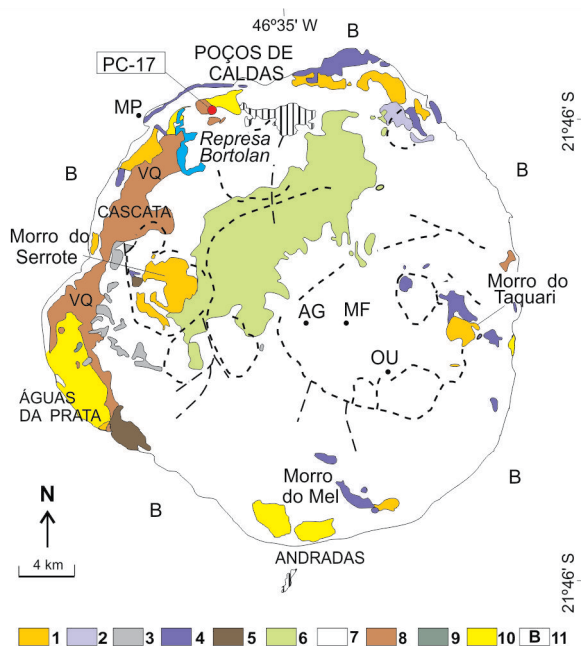


Figure 1. Simplified geological map of the Poços de Caldas alkaline massif (Ulbrich *et al.* 2002, 2005). Legend: NeS: Agpaite nepheline syenites; 1: pseudoleucite NeS; 2: porphyritic NeS; 3: grey NeS; 4: biotite-bearing NeS; 5: Pedreira type NeS; 6: undifferentiated tinguaites and phonolites; 7: volcanoclastic deposits emphasizing the Vale do Quartel strip; 8: diabase from the Serra Geral Formation; 9: sandstones from the Botucatu Formation and related sedimentary rocks from the Paraná Basin; 10B: undifferentiated igneous and metamorphic country rocks; AG: Campo Agostinho; MF: Morro do Ferro; MP: Minas Pedras quarry; OU: Osamu Utsumi open pit; VQ: Vale do Quartel. Heavy lines: fractures and faults; dotted lines: geomorphological circular structures. PC-17: collection site of the studied breccia samples.

showing a radial drainage pattern, a geomorphological feature probably associated with tinguaites forming dome-like intrusions. The largest one (the “central-eastern circular structure”) occupies an area of over a hundred square km, and concentrates, in its interior and along its outer limits, most of the mineral deposits that dot the district (caldasite occurrences, the Osamu Utsumi open pit mine, the Campo de Agostinho strip with U deposits, *cf.* Paradella & Almeida Filho 1976, Ulbrich *et al.* 2005, and Fig. 1). The hydrothermal alteration is homogeneously distributed throughout the district and is characterized by pyrite, recrystallized K-feldspars, and sericite (altered nepheline); mafic minerals are converted into oxides-hydroxides. The disappearance of pyrite and the increase in kaolinite contents signal the onset of supergene alteration (Garda 1990).

The N-S running Vale do Quartel structure (Fig. 1) is filled in with several types of pyroclastic rocks, specially constituted by mafic to ultramafic varieties (“ankaratrites”), according to Ellert (1959), as well as broken fragments of both country and the main types of Poços de Caldas rocks (Alves 2003). These mafic/ultramafic rocks constitute a separate genetic lineage, as documented by petrographic and chemical-isotopic data, in contrast to the feldspathic lineage, represented by the predominant Poços de Caldas felsic rocks (Ulbrich *et al.* 2005).

Country rocks are mostly basement granitic, gneissic and charnockitic rocks, as well as sedimentary cover formations, represented by sandstones from the Lower Cretaceous Botucatu Formation of the Paraná Basin, still preserved at the border areas of the massif, and, to a lesser extent, by some minor outcrops of the Serra Geral Formation diabases (Fig. 1).

Stratigraphy and geochronology

Geological observations indicate time gaps between the emplacements of different rock types in the massif. The Vale do Quartel pyroclastics and associated mafic-ultramafic rocks are closely related to the emplacement of the Poços de Caldas rocks themselves. Similar rock types are also observed cutting across basement and alkaline rocks (plugs and dikes), found both within (*e.g.*, lamprophyre dikes in the Osamu Utsumi open pit; *cf.* Shea 1992, Garda 1990) and outside of the massif (*e.g.*, Minas Pedras ultramafic lamprophyres and silico-carbonatite rocks, Vlach *et al.* 1996, 1998, 2003, Ulbrich *et al.* 2002), as well as isolated tuff and breccia outcrops found in assorted regional locations, some within the district. The breccia outcrops were identified as erosion remnants of a pyroclastic apron that probably covered the entire massif and was coeval with the main eruption episodes (*e.g.*, Björnberg 1959, Oliveira *et al.* 1975).

The majority of tinguaites are invaded by NeS varieties. Characteristics reminiscent of commingling structures are,

however, observed (*e.g.*, fine-grained tinguaites enclaves in the Pedreira NeS type, *cf.* Fig. 1) leading to a common interpretation that both rock types were roughly coeval and intruded as partly or mostly liquid magmas at the emplacement site (Ulbrich *et al.* 2002, 2005). Some late tinguaites cut across the NeS, as observed in the Pedreira da Prefeitura quarry (Fig. 1). The agpaitic NeS varieties are certainly somewhat younger than the coarse- and fine-grained, intermediate-miaskitic, rock varieties. In fact, khibinites are clearly intrusive in the northern-rim grey NeS, and both khibinites and lujavrites contain tinguaites xenoliths (Ulbrich 1984, Ulbrich *et al.* 2005).

The first attempts at K/Ar dating of alkaline rocks from Poços de Caldas were made by Amaral *et al.* (1967) and Bushee (1971), using mineral separates (mica, K-feldspar) and whole-rock samples from both feldspathic and mafic-ultramafic rocks, in a total of 40 determinations. The results, calculated with reference to the last recommended K decay constants, listed in Sonoki and Garda (1988), point to a large age span for the eruption history, from *ca.* 54 Ma (a NeS) to over 89 Ma (an ankaratrite).

Ulbrich *et al.* (2002) and Shea (1992) presented the first obtained results with the Rb/Sr dating method, considering conventional, internal, as well as reference isochrons. Ulbrich *et al.* (2002) reported isochrons of about 83 (± 21) Ma for the northern lujavrite-khibinite body and 89 (± 8), Ma for the northern grey NeS (see detailed map in Ulbrich & Ulbrich, 2000). Shea presented isochronic ages of about 79 (± 7) Ma for the Pedreira type NeS and 77 (± 3) Ma for hydrothermally altered NeS from a borehole in the Osamu Utsumi open pit. The same author also reported the first $^{40}\text{Ar}/^{39}\text{Ar}$ ages, dating phlogopites concentrates from mica lamprophyre dikes in the open pit, which yielded 75.7 (± 0.6) Ma (phlogopite phenocrysts) and (76 ± 2) Ma (groundmass phlogopite).

Ulbrich *et al.* (2002) reviewed all these results in light of the available geological and geomagnetic data and suggested that the main magmatic episodes in the Poços de Caldas massif occurred in a relatively short age span (1 to 2 Ma) at about 79 Ma, emphasizing, however, the discrepancies between the age results and the geomagnetic reversals. Thompson *et al.* (1998) suggested a somewhat larger intrusion interval, between 80 and 85 Ma. Vlach *et al.* (2003) reported an $^{40}\text{Ar}/^{39}\text{Ar}$ age of 83.9 (± 0.3) Ma in phlogopite concentrates from a calcite-phlogopite-fluorite late vein associated with the ultramafic rocks from the Minas Pedras quarry.

SAMPLING AND ANALYTICAL METHODS

Fresh samples of conduit breccia were collected years ago along the Águas da Prata — Poços de Caldas highway,

which runs along with the Vale do Quartel. Two samples from the same continuous outcrop (PC-17, Fig. 1), one with melanite-bearing NeS fragments, the other bearing phlogopite macrocrysts, were chosen for this study.

Sample preparation, petrographic and geochemical analytical works were carried out at the GeoAnalitica-USP core facility. $^{40}\text{Ar}/^{39}\text{Ar}$ phlogopite dating was done at the UQ-AGES Laboratory of the University of Queensland, Australia.

Both conventional and large polished thin sections were examined under transmitted and reflected light with a conventional petrographic microscope. Backscattered electronic images (BSE), qualitative energy, and quantitative wavelength dispersive spot analysis (EDS, WDS) were done with the JEOL FXA FE-8530 EPMA with 5 WD and 1 ED spectrometers. Analytical conditions for WDS analyses were 15 kV and 20 nA for the column accelerating voltage and beam current, respectively. Beam diameter was set to 5 μm for pyroxene, garnet and mica, and enlarged to 10–15 μm in the case of the alkali-feldspars. Standard analytical routines available in the lab were employed (*e.g.*, Gualda & Vlach 2007), and both synthetic and natural minerals (mainly from the Smithsonian collection) were used as standards. Matrix effect corrections and data reduction were performed with the PRZ/Armstrong scheme. Cationic proportions, structural formulae and $\text{Fe}^{3+}/\text{Fe}^{2+}$ partitions were computed using the MinCal software (*e.g.*, Gualda & Vlach 2005) and considering 32, 24, 22 and 6 O in the formula unit of feldspar, garnet, mica and pyroxene, respectively. Garnet end members were recast following Locock (2008).

$^{40}\text{Ar}/^{39}\text{Ar}$ dating routine followed the procedures established by Vasconcelos *et al.* (2002, see details in the Supplementary Materials). Samples were irradiated at the Cadmiun-lined B-1 CLICIT facility (Oregon State University, USA). Data were corrected for nucleogenic interferences, atmospheric contamination and mass discrimination, considering $^{40}\text{Ar}/^{39}\text{Ar} = 298.6 (\pm 0.3)$ in atmospheric argon (Renne *et al.* 2009). Ages were calculated using decay constants established by Steiger and Jäger (1977) at a 95% confidence level. The GA1550 (MD2) biotite standard, with a 98.5 ± 0.5 Ma recommended age (McDougall & Wellman, 2011), was analyzed simultaneously; two aliquots averaged 99.7 ± 0.5 Ma (age-probability spectrum, MSWD = 1.65, $P = 0.04$, $N = 19$).

PETROGRAPHY OF THE STUDIED SAMPLES

General field and petrographic aspects of the magmatic breccia types related to the evolution of the Poços de Caldas massif were presented by Ellert (1959), Ulbrich (1984, see

also Ulbrich 1986), and Alves (2003). Here we present a brief petrographic characterization of the studied conduit breccia samples, emphasizing their melanite-bearing NeS fragments and the phlogopite megacrysts.

The conduit breccias have typically grayish-green to dark green colors and are heterogeneous from outcrop to outcrop with respect to dimensions, abundance, and type of mineral and rock-fragment contents; the mineral fragments are always more abundant. They are polimictic and mostly clast-supported, with modal fragment volumes higher than *ca.* 75–80%. Two main contrasting varieties were recognized: the first one is a fine-grained variety with large amounts of reddish-brown mica (phlogopite) megacrysts (up to 2 cm), which also contains smaller rock fragments, while the second contains larger and more abundant rock fragments and fewer and smaller mica megacrysts.

In our samples, the rock fragments are made up of plutonic and volcanic/subvolcanic igneous rock varieties with a medium- to high-grade alteration, as well as sandstones from the Botucatu Formation. Their dimensions vary from less than one cm to several cms (rarely over a decimeter in outcrops) and they have subrounded to angular shapes. The medium- to coarse-grained igneous rocks include granite, quartz-feldspar gneiss, and charnockite types from the crystalline basement, as well as syenite varieties from the alkaline massif itself. Volcanic-subvolcanic types are made up of ankaramite-like mafic-ultramafic varieties with pyroxene microcrysts in a fine-grained matrix, basaltic rocks, probably related to the Serra Geral Formation (Fig. 2A), and some unidentified, dark-colored, aphanitic varieties. Alves (2003) also reported the presence of pyrochlore-bearing carbonate fragments in neighboring outcrops.

Quartz and feldspar (0.2–8.0 mm) are predominant among mineral fragments (Fig. 2A). The quartz grains have mostly rounded contours and show both regular and strong undulatory extinction. Feldspar grains have rounded and subidiomorphic contours, and include well-twinned, exsolution-free, fresh microcline, Carlsbad twinned homogeneous and mesoperthitic alkali-feldspar, and partially altered, both deformed and undeformed, plagioclase. Among the mafic minerals, phlogopite is observed as larger crystals (see description below and Fig. 2A), accompanied by smaller (< 1.0 mm), idiomorphic to subidiomorphic, pale brown augite and titanian augite, the latter with anomalous interference colors and some colorless diopsidic cores, as well as yellow-green aegirine-augite, partially substituted by carbonate. Carbonate, as fragments and recrystallized grains, occurs associated with aegirine-augite and aegirine. Rarely, minute and rounded zircon and monazite crystals may be seen.

The breccia matrix is very fine-grained and imprints a green color on the samples. Calcitic carbonate is detected

through reaction with dilute HCl in hand specimens, but most of its constituents are generally not recognizable even under the optical microscope. XRD analysis of a ground-mass concentrate points to the occurrence, besides calcite, of aegirine, arfvedsonite and some unidentified phyllosilicate; quartz and K-feldspar reminiscent of the mineral fragments were also detected.

Melanite-bearing nepheline syenite fragments

The melanite-bearing NeS fragments are greyish to slightly reddish-grey, angular to slightly rounded, and measure up to 4 cm (Fig. 2B). They are medium- to coarse-grained and

present a massive structure. In thin-polished sections, the contacts between fragments and the groundmass are sharp. Flow structures are observed around the fragments in some places. Modal contents vary: alkali-feldspar up to 65%, pseudomorphs after nepheline up to 30%, clinopyroxene up to 15%, and melanite garnet up to 5%. The main accessory is apatite (up to 1%). All fragments present intense late alteration and the secondary minerals may amount to up to 40%.

K-feldspar (2.5–5.0 mm) forms subidiomorphic to xenomorphic tabular to irregular crystals, sometimes Carlsbad-twinned, with irregular mutual contacts. Intense substitution by clay minerals, carbonate, hematite and white mica give most grains a clouded aspect. Rare clean and fresh surfaces

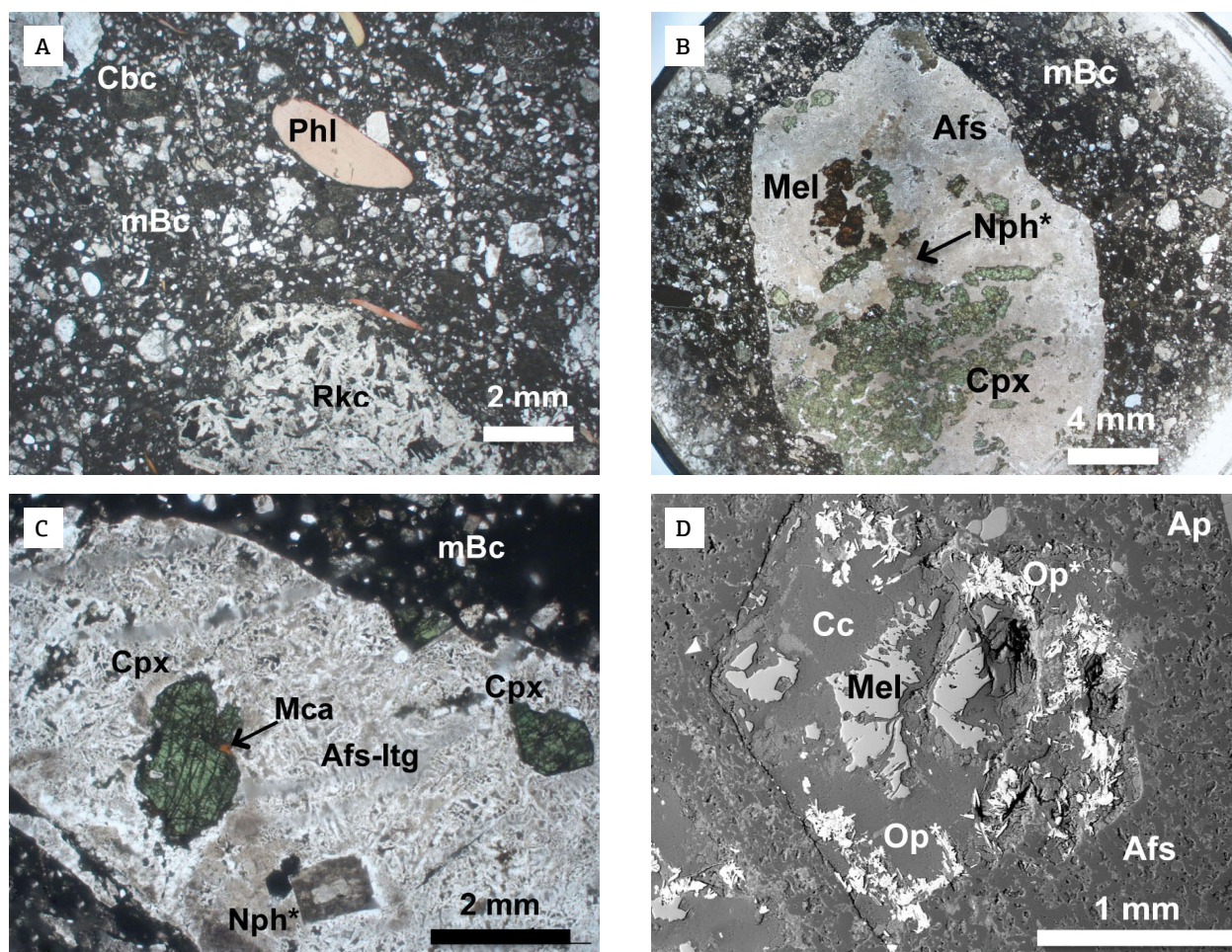


Figure 2. Plane polarized transmitted light (TL) and backscattered (BSE) electronic images of the studied breccia samples. (A) General aspect of the conduit breccia, showing fine-grained (mBc) portions with quartz, feldspar and pyroxene-predominant crystal fragments in a dark matrix, phlogopite megacrysts (Phi) with rounded contours, carbonate fragments (Cbc) with an aegirine-augite crystal and an intergranular-textured, basaltic-like rock fragment (Rkc); (B) a melanite-bearing NeS fragment with alkali-feldspar (Afs), nepheline pseudomorphs (light-brown, Nph*), clinopyroxene (Cpx) and melanite (Mel); (C) melanite-bearing NeS fragment, showing alkali-feldspar-nepheline(?) intergrowths, nepheline pseudomorphs, clinopyroxene and reddish mica substituting for pyroxene; (D) BSE image showing partially substituted idiomorphic melanite crystal, Cc: calcitic carbonate, Op*: (all of the brightest crystals in the image; include: ilmenite, sulphides and minor unidentified opaque phases), Ap: idiomorphic apatite crystal. See discussion in the text.

are homogeneous and free of exsolved phases. The alteration patterns observed in some crystals suggest some kind of previous intergrowths between feldspar and nepheline (Fig. 2C), resembling former pseudo-leucite aggregates (*e.g.*, Rogova 1966, Ruberti *et al.* 2012). Albite appears as late, pristine, interstitial xenomorphic crystals.

Quadrangular and rectangular pseudomorphs (up to 3.0 mm) with idiomorphic outlines and relict orthogonal cleavage traces, composed mainly of thin white mica and some carbonate, are interpreted as former nepheline crystals (Fig. 2C).

Idiomorphic to subidiomorphic clinopyroxene (up to 2.5 mm) appears as crystal clusters or isolated grains showing a green to yellow-green pleochroism, and a slightly irregular patchy zoning. Carbonate and orange-reddish mica (Fig. 2C) are substitution products and occur along cleavage planes and as thin outer zones.

Melanite (up to 1.5 mm) is idiomorphic to subidiomorphic and shows strong oscillatory zoning patterns accompanying its crystal faces. It is reddish-orange to dark red in color and presents variable alteration. Crystals form small clusters or appear isolated and are often associated with pyroxene (Fig. 2B). Alteration is strongest over the darkest crystal zones. The main substituting phases are calcite (dominant) and Fe-Ti oxides (mainly ilmenite); titanite, pyrite, chalcopyrite, and some other unidentified phases appear in trace quantities (Fig. 2D). In some places, just pseudomorphs after garnet, made up of these late phases, are observed.

The main accessory is apatite (up to 0.7 mm), which occurs as pristine fresh idiomorphic crystals. Rare opaque phases appear in some fragments.

Phlogopite megacrysts

Phlogopite is the easiest recognizable mafic mineral in breccia hand samples. Under the microscope, it appears as slightly deformed, pristine, and inclusion-free megacrysts, typically with rounded contours and reddish to yellowish-orange pleochroic colors. Deformation is best evidenced in sections normal to the cleavage, as crystals or crystal aggregates may appear bent around other mineral or rock fragments. Minute crystals made up of Fe-Ti oxides, mainly magnetite, armor some megacrysts. This late feature, and the rounded mica contours suggest the occurrence of emplacement-related absorption reaction and oxidation phenomena.

MINERAL CHEMISTRY

Quantitative WDS spot analyses were obtained for alkali-feldspars, clinopyroxene, melanite and late phlogopite from the rock fragments, as well as for the phlogopite macrocrysts.

Representative compositions are shown in Table 1. The complete data set is available in the Supplementary Materials. The main chemical signatures of each mineral phase are described in the following paragraphs.

Alkali-feldspars

The primary alkali-feldspar has a relatively homogeneous composition, varying in the $Or_{83}Ab_{17}$ - $Or_{95}Ab_{05}$ range, with low An (≤ 0.6 mol) contents (Tab. 1, Fig. 3). Fe, Sr and Ba contents are low: ≤ 0.08 , ≤ 0.08 , and ≤ 0.12 cpfu (cations per formula unit), respectively (Tab. 1). Sr and Ba show a slightly negative correlation with K. Of note, these compositions strongly contrast with those measured in alkali-feldspar from the Pedreira NeS facies, which are characterized by very high Sr contents (SrO up to 1.4 wt.%, *cf.* Ulbrich 1983, 1993).

Secondary albite, formed probably by late exsolution reactions, is almost pure, with Ab ≥ 97.5 mol% (Fig. 3), and low Or (≤ 2.7) and An (≤ 0.8) molecular contents. Fe, Sr and Ba occur in trace amounts.

Clinopyroxene

The clinopyroxene compositions (Tab. 1, Fig. 4A) plot mainly as diopside, with some minor hedenbergite and augite compositions in the quadrilateral scheme of Morimoto (1988). Of importance, the classic pyroxene classification (*e.g.*, Deer *et al.* 1978) uses the names salite and sodian salite (instead of diopside), sodian ferrosalite (instead of hedenbergite) and sodian augite (instead of augite), which have better petrologic meaning. They are characterized by $0.44 \leq mg\# \leq 0.65$, low to moderate Al ($0.04 \leq Al^T$ (cpfu) ≤ 0.16) and a significant acmite molecular content (up to 11.1%, see Tab. 1).

The compositional variations observed in our data set are well described by the substitution vector $[M^{2+}]_2[NaFe^{3+}]$ as depicted in Figure 4B, a feature typically observed in common Ca-rich pyroxenes of alkaline igneous rocks (*e.g.*, Deer *et al.* 1978).

Garnet

The analyzed titanian garnet presents $0.274 \leq Ti \leq 0.596$, $0.020 \leq Zr \leq 0.144$, $Al^T \leq 0.451$ (cpfu), and $0.85 \leq Fe^{3+}/(Fe^{2+}+Fe^{3+}) \leq 0.98$ (Tab. 1). As mentioned, the darker zones within melanite crystals were the most susceptible to late alteration, thus Ti(Zr) compositions richer than those measured probably did exist. When compared with several compositions published in the literature (*e.g.*, Deer *et al.* 1982), our melanite structural formulae fit better considering that most Fe^{2+} fills in octahedral, rather than dodecahedral sites.

The main molecular garnet end members, according to Locock (2008), as shown in Table 1 (see also

Supplementary Material), are andradite [Andr, $\text{Ca}_3\text{Fe}^{3+}_2\text{Si}_3\text{O}_{12}$, up to 85%], morimotoite [Mrmt, $(\text{CaFe}^{2+})_3\text{Ti}(\text{Mg},\text{Fe}^{2+})\text{Si}_3\text{O}_{12}$, up to 19%], schorlomite [Schrlm, $\text{Ca}_3\text{Ti}_2\text{Si}(\text{Fe}^{3+},\text{Al})_2\text{O}_{12}$, up to 10%], kimzeyite [Kimz, $\text{Ca}_3\text{Zr}_2\text{SiAl}_2\text{O}_{12}$, up to 4%] and the hypothetical *NaTi garnet* [NaTiGrt, $\text{Na}_2\text{CaTi}_2\text{Si}_3\text{O}_{12}$, up to 2.5%]. It is worth noting that Antao (2014), on the basis of structural refinement results, shows that morimotoite and schorlomite are very similar mineral species. The observed compositional variations are well represented in the ternary diagrams Andr-Schrlm-Mrmt and Mrmt-Kimz-Schrlm, as depicted in Figure 5. Zr has a strong negative correlation with Al in our data set, resulting in a progressive increase of the Kinz molecule as Schrlm decreases, as evidenced in Fig. 5.

Ti and Zr, because of their crystallochemical properties, are expected to substitute Si in the melanite tetrahedral sites. However, in general, they are mainly partitioned into octahedral coordination, and enter into the garnet structure through the coupled substitution defined by the vector $[\text{R}^{3+}]_2 [(\text{Ti},\text{Zr})(\text{R}^{2+})]$, as suggested by Grapes et al. (1979).

Micas

Both the micas constituting the breccia megacrysts and the late crystals in the melanite-bearing NeS breccia fragments have relatively homogeneous chemical compositions (Tab. 1). They are classified and compared in the triangular diagram $\text{Mg}-\text{Al}^{\text{T}}-(\text{Fe}^{2+}+\text{Mn})$ in Fig. 6.

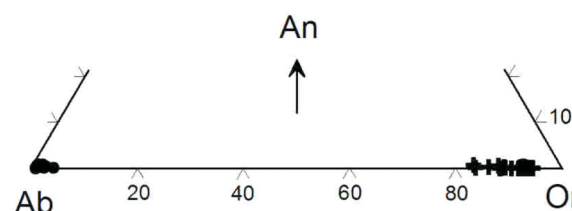


Figure 3. Ternary molecular Albite-Anortite-Orthoclase feldspar diagram showing the compositional variations of primary K-feldspar and late albite in melanite-bearing NeS fragments from the Poços de Caldas conduit breccia.

Table 1. Representative chemical compositions (WDS quantitative spot analysis) of alkali-feldspars, clinopyroxene, garnet and late mica from the melanite-bearing NeS fragments, and of phlogopite megacrysts from the Poços de Caldas conduit breccia. n.a. = not analyzed, b.d. = below detection limit. mg# = cationic $\text{Mg}/(\text{Mg} + \text{Fe}^{2+} + \text{Mn})$. See text for discussion, and the Supplementary Material for the complete data set.

| Mineral | K-feldspar | | Late Albite | Clinopyroxene | | | Melanite Garnet | | | | Megacrystic Phlogopite | | | Late Mica | |
|-------------------------|------------|--------|-------------|---------------|--------|-------|-----------------|--------|-------|-------|------------------------|-------|-------|-----------|-------|
| Point ID | 02.1.5 | 02.1.9 | 02.01.9a | c.1.1 | c.2.1 | b.2.1 | i1.1 | i.2.1 | b.2.1 | i.3.2 | c1.c | c2.i | c3.c | p.1 | p.2 |
| SiO_2 | 64.50 | 64.73 | 68.31 | 51.22 | 51.30 | 50.89 | 33.68 | 34.27 | 35.40 | 33.92 | 37.69 | 37.95 | 37.21 | 41.07 | 38.37 |
| TiO_2 | b.d. | b.d. | 0.02 | 0.47 | 0.63 | 0.28 | 3.86 | 3.50 | 2.22 | 2.75 | 6.39 | 6.62 | 6.51 | 0.40 | 1.82 |
| ZrO_2 | n.a. | n.a. | n.a. | n.a. | n.a. | n.a. | 1.21 | 0.22 | 0.15 | 0.29 | n.a. | n.a. | n.a. | n.a. | n.a. |
| Al_2O_3 | 19.19 | 18.45 | 19.68 | 1.25 | 1.49 | 0.94 | 1.43 | 2.08 | 2.22 | 1.95 | 16.11 | 16.11 | 15.80 | 9.56 | 12.87 |
| Cr_2O_3 | n.a. | n.a. | n.a. | n.a. | n.a. | n.a. | b.d. | b.d. | b.d. | b.d. | n.a. | n.a. | n.a. | n.a. | n.a. |
| FeO^{T} | 0.23 | 0.35 | 0.21 | 11.74 | 13.47 | 17.26 | 24.18 | 23.98 | 24.23 | 24.12 | 6.36 | 6.59 | 9.81 | 14.54 | 16.70 |
| MnO | b.d. | b.d. | b.d. | 0.58 | 0.68 | 0.70 | 0.55 | 0.50 | 0.44 | 0.44 | 0.04 | 0.04 | 0.06 | 0.48 | 0.56 |
| MgO | 0.02 | 0.00 | 0.00 | 10.81 | 9.60 | 7.57 | 0.21 | 0.23 | 0.20 | 0.21 | 18.53 | 18.55 | 16.31 | 19.88 | 15.53 |
| ZnO | n.a. | n.a. | n.a. | n.a. | n.a. | n.a. | n.a. | n.a. | n.a. | n.a. | b.d. | b.d. | b.d. | 0.08 | 0.08 |
| CaO | b.d. | b.d. | 0.03 | 22.35 | 21.52 | 18.91 | 31.67 | 32.08 | 32.42 | 32.18 | 0.00 | 0.08 | 0.05 | 0.12 | 0.24 |
| SrO | b.d. | 0.05 | 0.04 | n.a. | n.a. | n.a. | n.a. | n.a. | n.a. | n.a. | n.a. | n.a. | n.a. | n.a. | n.a. |
| BaO | 0.02 | b.d. | 0.03 | n.a. | n.a. | n.a. | n.a. | n.a. | n.a. | n.a. | 0.25 | 0.23 | 0.26 | b.d. | 0.11 |
| Na_2O | 1.85 | 0.72 | 11.66 | 1.19 | 1.49 | 3.00 | 0.10 | 0.19 | 0.16 | 0.15 | 0.12 | 0.15 | 0.16 | b.d. | 0.14 |
| K_2O | 14.53 | 15.75 | 0.18 | b.d. | b.d. | 0.09 | n.a. | n.a. | n.a. | n.a. | 10.24 | 10.17 | 10.11 | 9.04 | 9.70 |
| F | n.a. | n.a. | n.a. | n.a. | n.a. | n.a. | n.a. | n.a. | n.a. | n.a. | b.d. | b.d. | b.d. | 0.30 | 0.18 |
| Cl | n.a. | n.a. | n.a. | n.a. | n.a. | n.a. | n.a. | n.a. | n.a. | n.a. | 0.02 | 0.04 | 0.01 | b.d. | b.d. |
| O(=F,Cl) | - | - | - | - | - | - | - | - | - | - | 0.01 | 0.01 | 0.00 | 0.12 | 0.08 |
| Sum | 100.39 | 100.06 | 100.17 | 99.60 | 100.17 | 99.64 | 96.88 | 97.05 | 97.47 | 96.03 | 95.75 | 96.52 | 96.30 | 95.35 | 96.23 |
| mg# | - | - | - | 0.61 | 0.55 | 0.43 | - | - | - | - | 0.84 | 0.83 | 0.75 | 0.70 | 0.62 |
| Molecular components | | | | | | | | | | | | | | | |
| Or | 83.73 | 93.51 | 1.52 | Wo | 45.47 | 44.26 | 38.67 | Kimz | 2.51 | 0.45 | 0.31 | 0.60 | | | |
| Ab | 16.20 | 6.49 | 98.23 | En | 30.60 | 27.47 | 21.54 | Schrlm | 4.14 | 5.29 | 1.82 | 5.17 | | | |
| An | 0.06 | 0.01 | 0.25 | Fs | 19.57 | 22.73 | 28.69 | Mrmt | 14.77 | 8.49 | 7.74 | 4.80 | | | |
| | | | | Ac | 4.36 | 5.55 | 11.10 | Gros | 0.00 | 2.08 | 6.40 | 2.56 | | | |
| | | | | | | | | Andr | 74.60 | 79.62 | 79.95 | 84.11 | | | |
| | | | | | | | | Others | 3.98 | 4.07 | 3.78 | 2.76 | | | |

The phlogopite megacrysts present a peculiar chemical composition, defined especially by high Ti (up to 0.71 cpfu) and Al (up to 2.75 Al^T cpfu). Mg contents are also high ($0.74 \leq \text{mg\#} \leq 0.85$), while Ba (≤ 0.02 cpfu) and F (≤ 0.01 cpfu) appear in trace concentrations. Cationic Ti contents show a strong positive correlation (not shown) with ^{IV}Al and negative correlations with the M²⁺ cations (Fe²⁺ + Mn, Mg) and Si, indicating that Ti cations enter the phlogopite

structure mainly through the substitution vector $[M^{2+} + 2Si]_{-1}[Ti^{4+} + 2^{IV}Al]_{+1}$, as modified from the original suggestion of Robert (1976, see also Arima and Edgar 1981). Based on experimental and crystallochemical evidence, these latter authors conclude that phlogopite Ti contents depend on temperature, pressure, and Oxygen fugacity (f_{O_2}).

The late mica, substituting for pyroxene in the melanite-bearing NeS fragments, presents $0.61 \leq \text{mg\#}$

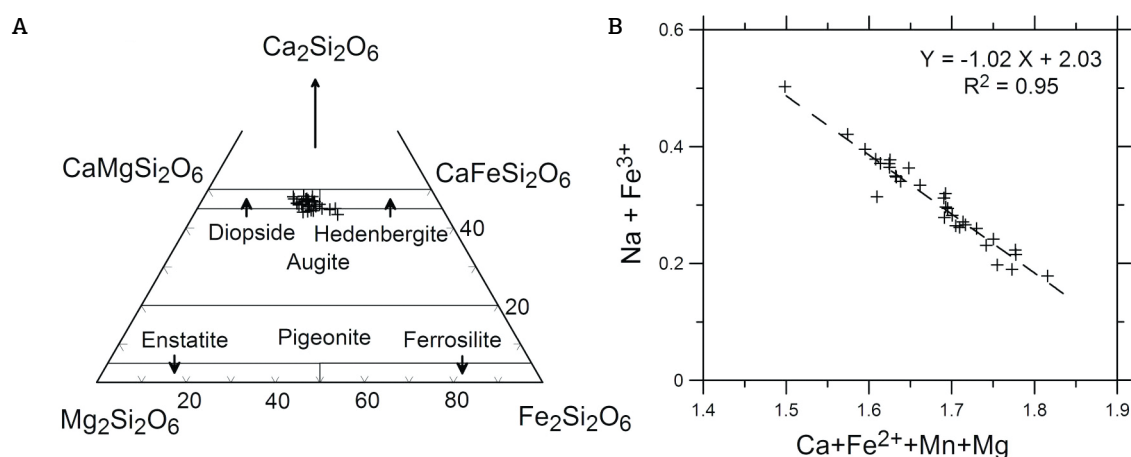


Figure 4. Compositional variations in clinopyroxenes of melanite-bearing NeS fragments from the Poços de Caldas conduit breccia. (A) Quadrangular Enstatite-Diopside-Hedenbergite-Ferrosilite [$Mg_2Si_2O_6$ - $CaMgSi_2O_6$ - $CaFeSi_2O_6$ - $Fe_2Si_2O_6$] diagram, with compositional field names as defined by Morimoto (1988, see text for discussion). (B) Compositional variations related by the $[Ca + Fe^{2+} + Mn + Mg]_{-1}[Na + Fe^{3+}]_{+1}$ coupled cationic substitution.

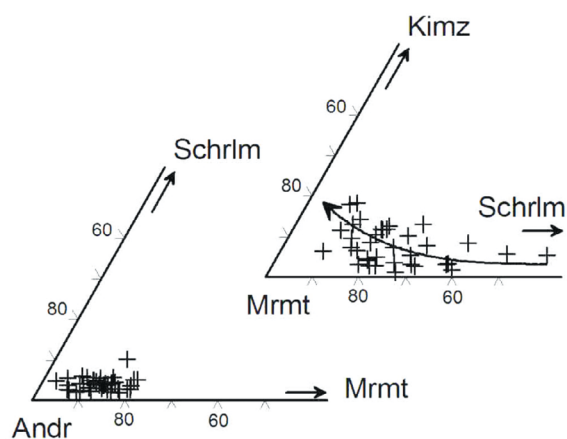


Figure 5. Compositional variations of garnet in the melanite-bearing NeS fragments from the Poços de Caldas conduit breccia plotted in ternary molecular diagrams. Molecular end members as defined by Locock (2008): Andradite, Andr [$Ca_3Fe^{3+}_2Si_3O_{12}$]; Kimzeyite, Kimz [$Ca_3Zr_2SiAl_2O_{12}$]; Morimotoite, Mrmt [$(CaFe^{2+})_3Ti(Mg,Fe^{2+})Si_3O_{12}$]; Schorlomite, Schrlm [$Ca_3Ti_2Si(Fe^{3+},Al)_2O_{12}$]. See text for discussion.

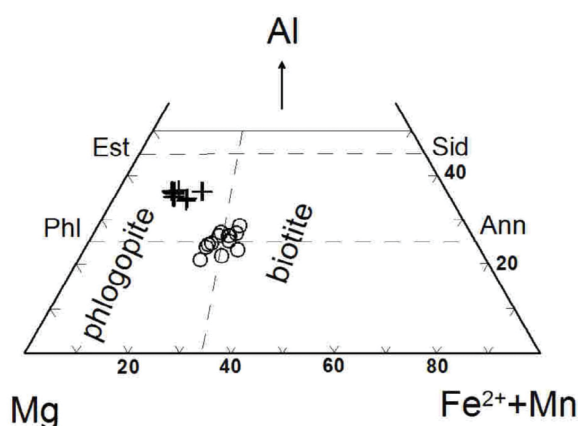


Figure 6. Compositional variations of phlogopite megacrysts and of late biotite and phlogopite from the melanite-bearing NeS fragments from the Poços de Caldas conduit breccia in the Mg-Al^T-(Fe²⁺+Mn) diagram. Molecular end members: Ann, Annite [$K_2Fe_6(Si_6Al_2O_{20})(OH)_4$]; Est, Eastonite [$K_2Mg_6Al_3(Si_4Al_4O_{20})(OH)_4$]; Phl, Phlogopite [$K_2Mg_6(Si_6Al_2O_{20})(OH)_4$]; Sid, Siderophyllite [$K_2Fe_4Al_2(Si_4Al_4O_{20})(OH)_4$]. Compositional fields as defined by Mitchell (1995). Symbols: crosses, breccia megacrysts; open circles, late mica from melanite-bearing NeS fragments.

≤ 0.70 and relatively low Al^T (1.68–2.28 cpdf). In fact, several analyses have $(Si+Al^T) < 8$ cpdf and some Fe^{3+} is needed to fill in the tetrahedral sites (see also Suppl. Tab. 1.). It also has low Ti (≤ 0.22 cpdf), Ba (≤ 0.01 cpdf) and F (≤ 0.19 cpdf) contents, and relatively high Ca (up to 0.05 cpdf) contents. The compositions plot in a transitional field between biotite and phlogopite, as defined by Mitchell (1995) and depicted in Fig. 6.

⁴⁰Ar/³⁹Ar DATING OF PHLOGOPITE MEGACRYSTS

Analytical isotope data for phlogopite concentrates from sample PC-17 (IBI-42q) are presented in full in the Supplementary Materials. Two megacryst aliquots were analyzed and yielded very similar results (Fig. 7). The step-heating spectra show well-defined age plateaus, compatible with closed systems, and give integrated ⁴⁰Ar/³⁹Ar ages of 87.1 (± 0.5) Ma and 86.6 (± 0.5) Ma, respectively. The combined age-probability spectrum peaks at 86.7 Ma, and indicates a probable ⁴⁰Ar/³⁹Ar age of 86.7 (± 0.4) Ma (MSWD = 1.35, $P = 0.14$, $N = 21$) for the isotopic system closure. The computed isochronic ³⁶Ar/⁴⁰Ar - ³⁹Ar/⁴⁰Ar age (86.6 ± 0.4 Ma, ⁴⁰Ar/³⁶Ar = 309 ± 14 , MSWD = 1.2, $P = 0.2$, $N = 25$, not shown) is almost identical and indicates strong internal data consistency.

This age is significantly older than the ⁴⁰Ar/³⁹Ar phlogopite ages reported for the late carbonatitic veins from the Minas Pedras quarry (*ca.* 84 Ma; Vlach *et al.* 2003) and for

the lamprophyre dike from the Osamu Utsumi open pit (*ca.* 76 Ma; Shea 1992), as summarized in section 2.1.

DISCUSSION AND SUMMARY

On the occurrence of melanite-bearing nepheline syenites and its petrologic implications

Melanite garnet occurs in several felsic to mafic-ultramafic alkaline rocks, such as metaluminous NeS, ijolites, melteigites, various lamprophyres and silico-carbonatite types, and their volcanic-subvolcanic equivalents (*e.g.*, Deer *et al.* 1982, Rock 1991, and references therein). In southern Brazil, its presence was previously described in several Mesozoic alkaline massifs (Gomes 1969, Brotzu *et al.* 1997, Ruberti *et al.* 2012).

Few reports exist regarding the presence of melanite in the Poços de Caldas Massif. The first mention came from the pioneering work of Machado (1888), who described the presence of melanite in a coarse-grained clinopyroxene NeS. The author studied many other minerals and rocks, supposedly collected within the massif, but did not provide enough information as to identify the exact collection sites. Bushee (1971) described an unusual occurrence of melanite in khibinites from the northern area of the massif, but our previous work showed that this mineral is sphalerite (G. Gualda and S. Vlach, pers. commun.) Thus, in the Poços de Caldas region, confirmed reports up to now indicate that melanite occurs in ultramafic lamprophyres and

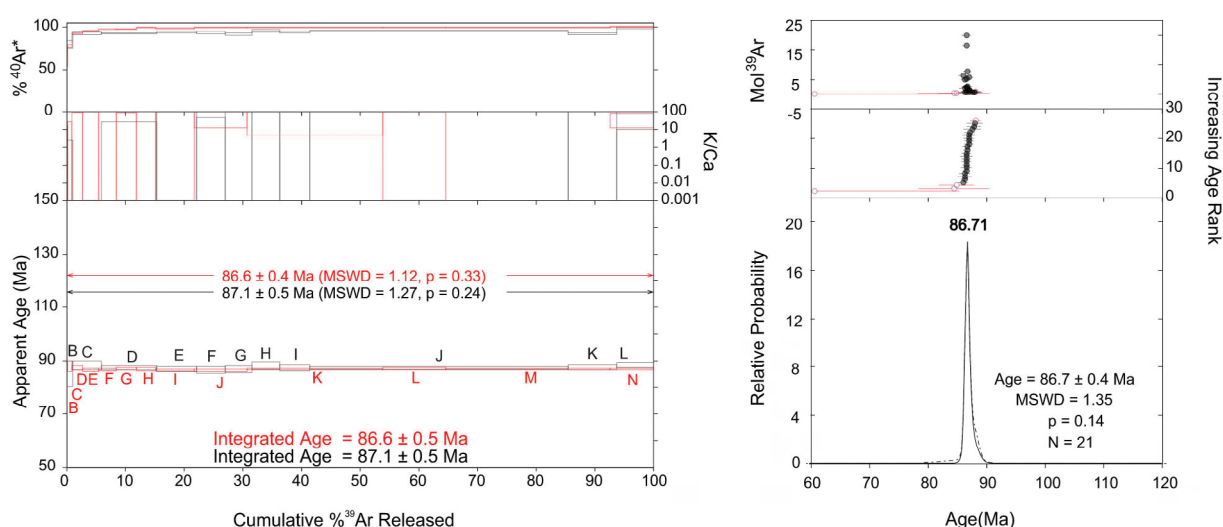


Figure 7. ⁴⁰Ar/³⁹Ar age diagrams for phlogopite megacrysts from the Poços de Caldas conduit breccia (Sample PC-17.1 = IBI-42q). Left: ⁴⁰Ar/³⁹Ar step heating spectra (colors represent results for the two analyzed aliquots); note the homogeneous plateaus and ages. Right: density probability plot, integrating age steps of both aliquots. See text for discussion.

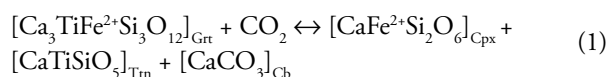
related silico-carbonatitic rocks at the Minas Pedras quarry (Vlach *et al.* 1996, 1988, Vilalva & Vlach 2004).

Typical metaluminous (miarctitic) NeS types are relatively rare in the district, a statement that apply also to tinguaites. However, detailed data for them are incomplete, available only for certain areas within the massif (Ulbrich 1983, Ulbrich *et al.* 2005, and references therein). In fact, the largest NeS intrusion, the Pedreira facies, outcropping in the central and northern area of the massif, is made up of moderately miarctitic, slightly metaluminous, as well as slightly peralkaline, types [$0.98 \leq [(Na_2O+K_2O)/Al_2O_3]_{molar} \leq 1.05$, cf. Ulbrich 1984, Ulbrich *et al.* 2005].

The rock fragments found in the conduit breccia point to the existence of hidden or unexposed NeS, with a marked metaluminous geochemical character in Poços de Caldas, a feature shared by several Brazilian and worldwide alkaline massifs.

Experimental data on the equilibrium of hedenbergite-andradite assemblages indicate that these minerals coexist under relatively high oxygen fugacities (f_{O_2} above the Ni-NiO buffer at $T \leq 650^\circ C$) in skarn-like natural systems (e.g., Gustafson 1974, Liou 1974, Moecher and Chou 1990). In mafic-ultramafic and feldspathic alkaline igneous rocks, however, Virgo *et al.* (1976) have shown that Ca-pyroxene and Ti-andradite could coexist well below the QFM (quartz-fayalite-magnetite) buffer.

Several metaluminous NeS contain melanite, with variable Ti contents, coexisting with Ca-pyroxene, titanite and primary calcitic carbonate (e.g., melanite-bearing pseudo-leucite syenites from the Banhadão Alkaline Complex, Ruberti *et al.* 2012). This mineralogical association may be constrained to some extent by the prevailing f_{CO_2} of the crystallizing environment, according to the following reaction, which is independent of f_{O_2} (Eq. 1):



This reaction suggests that the presence and increase of the morimotoite molecular component in garnet is favored by relatively low f_{CO_2} . It could help constrain the presence of Ti-garnets in CO_2 -bearing alkaline feldspathic as well as silico-carbonatite systems, like those appearing at the Minas Pedras quarry.

Phlogopite megacrysts compositions, age, and implications

The chemical fingerprints of the studied phlogopite megacrysts, especially the relatively high contents of Al, Ti, and Mg, are common features of phlogopites from worldwide occurrences in lamprophyric rocks, as well as some carbonatites, kimberlite, and other related types (e.g., Rock 1991, Mitchell 1995, and references therein). Thus, our measured compositions do not provide

a diagnostic chemical characterization that would undoubtedly tie mineral chemistry to rock association. For instance, chemically similar phlogopites, both with relatively high and low Ba and F contents, were described in samples from the ultramafic lamprophyres and related silico-carbonatites from the Minas Pedras quarry (Vlach *et al.* 1996, 2003).

Textures in the phlogopite megacrysts suggest that they are pieces torn off from still crystallizing magma mushes from an unknown depth, rather than fragments of solid rocks. In fact, they are not highly deformed or broken up, as would be expected if they had been subjected to a violent explosion of a host solid media. Our chemical data, as well as the occurrence of augite/Ti-augite companion crystal fragments, suggest a source akin to magmatic systems associated with ultramafic lamprophyres, silico-carbonatites, and ankaratrites, such as those cropping out in the Minas Pedras quarry and the Vale do Quartel area.

The obtained $^{40}Ar/^{39}Ar$ age (ca. 87 Ma) should represent a *minimum age* for phlogopite crystallization and formation of melanite-bearing NeS and other hosted fragments as well as a *maximum age* for breccia emplacement. Considering the relatively shallow crustal emplacement levels involved, such minimum and maximum values are expected to be similar, within error estimates. This age is somewhat older than the $^{40}Ar/^{39}Ar$ age available for the carbonatite late veins in the Minas Pedras quarry (ca. 84 Ma, Vlach *et al.* 2003) and the Rb/Sr isochron reported for the lujavrite-khibinite body (ca. 83 Ma, Ulbrich *et al.* 2002, 2005), and somewhat younger than a whole-rock K/Ar age obtained for an ankaratrite (Bushee 1971, Sonoki & Garda 1988) as well as the Rb/Sr isochron for the northern NeS (ca. 89 Ma, cf. Ulbrich *et al.*, 2002, 2005). It should be noted that all of them are significantly older than the “best” presumed (ca. 79 Ma) age for the main magmatism of the massif according to Ulbrich *et al.* (2002).

Geomagnetic data may give some important clues. The “33” geomagnetic reversal period spans from 73.6 to 83.0 Ma (cf. Cande & Kent 1995, Ulbrich *et al.* 2002, 2005) and helps to verify the consistency of the available age data set. The Poços de Caldas feldspathic rocks present a reverse (r) polarity, while three analyzed mafic-ultramafic rock samples from the Vale do Quartel area show normal (n) magnetization (Montes Lauar 1988). This data set would suggest that the feldspathic Poços de Caldas rocks would be placed into the 33r period (79.1 to 83 Ma), while the mafic-ultramafic types (which are younger, since they cut the feldspathic rocks, also providing breccia fragments), should be placed within the 33n (73.6 to 79.1 Ma), a younger period. In this context, the ages of the mafic-ultramafic rocks over this time interval may present a problem, as they reveal significant discrepancies between the geomagnetic reversal time-scale and the available dating

results. Ongoing detailed geochronological work would help solve such a conundrum.

ACKNOWLEDGEMENTS

We thank the staff of the GeoAnalítica-USP (São Paulo, Brazil) core facility and the IQ-Ages Laboratory (Queensland, Australia) for analytical support, Ms. M. Arroyave for imaging help, and Fundação de Amparo à Pesquisa do Estado de São Paulo (FAPESP, Thematic Project No 2012/06082-6, Coord.

E. Ruberti) for financial support. H. Ulbrich and M. Ulbrich would like to thank FAPESP for previous grants that allowed for field and laboratory work on the Poços de Caldas massif for several years. Lastly, the suggestions and criticism from G. Gualda and an anonymous reviewer were much appreciated.

SUPPLEMENTARY DATA

Supplementary data associated with this article can be found in the online version: [Supplementary Table 1](#).

REFERENCES

- Almeida F.F.M. 1983. Relações tectônicas das rochas alcalinas mesozóicas da região meridional da plataforma sul-americana. *Revista Brasileira de Geociências*, **13**:139-158.
- Alves A.D. 2003. *Rochas Vulcanoclásticas do Complexo Alcalino de Poços de Caldas - MG/SP*. MS Dissertation, Instituto de Geociências, Universidade de São Paulo, São Paulo, 106 p.
- Amaral G., Bushee J., Cordani U.G., Kawashita K., Reynolds J.H. 1967. Potassium-argon ages of alkaline rocks from southern Brazil. *Geochimica et Cosmochimica Acta*, **31**:117-142. [https://doi.org/10.1016/S0016-7037\(67\)80041-3](https://doi.org/10.1016/S0016-7037(67)80041-3)
- Antao S.M. 2014. Schorlomite and morimotoite: what's in a name? *Powder Diffraction*, **29**:346-351. <https://doi.org/10.1017/S0885715614000529>
- Arima M., Edgar A.D. 1981. Substitution mechanisms and solubility of titanium in phlogopites from rocks of probable mantle origin. *Contributions to Mineralogy and Petrology*, **77**:288-295. <https://doi.org/10.1007/BF00373544>
- Björnberg A.J.B. 1959. Rochas clásticas do Planalto de Poços de Caldas. *Boletim Faculdade de Filosofia, Ciências e Letras, Universidade de São Paulo, Geologia*, **237**(18): 65-123.
- Brotzu P., Gomes C.B., Melluso L., Morbidelli L., Morra V., Ruberti E. 1997. Petrogenesis of coexisting SiO₂-undersaturated to SiO₂-oversaturated felsic igneous rocks: The alkaline complex of Itatiaia, southeastern Brazil. *Lithos*, **40**:133-156. [https://doi.org/10.1016/S0024-4937\(97\)00007-8](https://doi.org/10.1016/S0024-4937(97)00007-8)
- Bushee J. 1971. *Petrographical and geochronological studies in alkaline rocks from southern Brazil*. PhD Thesis, The University of California, Berkeley, 145 p.
- Cande S.C., Kent D.V. 1995. Revised calibration of the geomagnetic polarity timescale for the Late Cretaceous and Cenozoic. *Journal of Geophysical Research*, **100**:6093-6095. <https://doi.org/10.1029/94JB03098>
- Comin-Chiaromonte P., Gomes C.B. 2005. *Mesozoic to Cenozoic Alkaline Magmatism in the Brazilian Platform*. São Paulo, EDUSP/FAPESP, 751 p.
- Deer W.A., Howie R.A., Zussman J. 1978. *Rock-forming minerals*, v. 2A: *Single-chain silicates*. 2nd. London, Longman Group Limited, 668 p.
- Deer W.A., Howie R.A., Zussman J. 1982. *Rock-forming minerals*, v. 1: *Orthosilicates*. New York, Longman Group Limited, 919 p.
- Derby O.A. 1887. On nepheline rocks in Brazil, with special reference to the association of phonolite and foyaite. *Quarterly Journal of the Geological Society of London*, **43**:457-473. <https://doi.org/10.1144/GSL.JGS.1887.043.01-04.35>
- Ellert R. 1959. Contribuição à geologia do Maciço Alcalino de Poços de Caldas. *Boletim da Faculdade de Filosofia, Ciência e Letras, Universidade de São Paulo*, **237**(18):5-63. <http://dx.doi.org/10.11606/issn.2526-3862.bffcluspgeologia.1959.121851>
- Garda G.M. 1990. *A alteração hidrotermal no contexto da evolução geológica do maciço alcalino de Poços de Caldas, MG-SP*. MS Dissertation, Instituto de Geociências, Universidade de São Paulo, São Paulo, 161 p.
- Gomes C.B. 1969. Electron microprobe analysis of zoned melanites. *American Mineralogist*, **54**:1654-1661.
- Grapes R.H., Yagi K., Okumura K. 1979. Aenigmatite, sodic pyroxene, arfvedsonite and associated minerals in syenites from Morou, Sakhalin. *Contributions to Mineralogy and Petrology*, **69**:97-103. <https://doi.org/10.1007/BF00371855>
- Gualda G.A.R., Vlach S.R.F. 2005. Stoichiometry-based estimates of ferric iron in calcic, sodic-calcic and sodic amphiboles: A comparison of various methods. *Anais da Academia Brasileira de Ciências*, **77**:521-534. <http://dx.doi.org/10.1590/S0001-37652005000300012>
- Gualda G.A.R., Vlach S.R.F. 2007. The Serra da Graciosa A-type granites and syenites, southern Brazil. Part II: Petrographic and mineralogical evolution of the alkaline and aluminous associations. *Lithos*, **93**:310-327. DOI: 10.1016/j.lithos.2006.06.002
- Gustafson W.I. 1974. The stability of andradite, hedenbergite, and related minerals in the system Ca-Fe-Si-O-H. *Journal of Petrology*, **15**:455-496. <https://doi.org/10.1093/petrology/15.3.455>
- Liou J.G. 1974. Stability relations of andradite-quartz in the system Ca-Fe-Si-O-H. *American Mineralogist*, **59**:1016-1025.
- Locock A.J. 2008. An Excel spreadsheet to recast analyses of garnet into end-member components, and a synopsis of the crystal chemistry of natural silicate garnets. *Computer Geosciences*, **34**:1769-1780. <https://doi.org/10.1016/j.cageo.2007.12.013>
- Machado J. 1888. Beitrag zur Petrographie der suedwestlichen Grenze zwischen Minas Gerais und São Paulo. *Tschermak's Mineralogische und Petrographische Mitteilungen*, **9**:318-360.
- McDougall I., Wellman P. 2011. Calibration of GA1550 biotite standard for K/Ar and ⁴⁰Ar/³⁹Ar dating. *Chemical Geology*, **280**:19-25. DOI: 10.1016/j.chemgeo.2010.10.001
- Mitchell R.H. 1995. *Kimberlites, orangeites, and related rocks*. New York, Plenum Press, 410 p.
- Moecher D.P., Chou I-M. 1990. Experimental investigation of andradite and hedenbergite equilibria employing the hydrogen sensor technique, with revised estimates of $\Delta fG^0_{m,298}$ for andradite and hedenbergite. *American Mineralogist*, **75**:1327-1341.

- Montes Lauar C.F. 1988. *Estudo paleomagnético dos maciços alcalinos de Poços de Caldas, Passa Quatro e Itatiaia*. MS Dissertation, Instituto Astronômico e Geofísico, Universidade de São Paulo, São Paulo, 101 p.
- Morimoto N. 1988. Nomenclature of pyroxenes. *Mineralogy and Petrology*, **39**:55-76. <https://doi.org/10.1007/BF01226262>
- Oliveira M.A.F., Alves F.R., Coimbra A.M. 1975. Sedimentação associada ao vulcanismo alcalino de Poços de Caldas (Divinolândia, SP). *Boletim do Instituto de Geociências da Universidade de São Paulo*, **6**:13-19.
- Paradella W.R., Almeida Filho R. 1976. Condicionamento das mineralizações radioativas no Planalto de Poços de Caldas baseado em imagens MSS de Landsat. In: *Congresso Brasileiro de Geologia*, 29., Ouro Preto. *Anais...* **3**:181-190.
- Renne P.R., Cassata W.S., Morgan L.E. 2009. The isotope composition of atmospheric argon $^{40}\text{Ar}/^{39}\text{Ar}$ geochronology: Time for a change? *Quaternary Geology*, **4**:288-298. DOI: 10.1016/j.quageo.2009.02.015
- Robert J.L. 1976. Titanium solubility in synthetic phlogopite solid solutions. *Chemical Geology*, **17**:213-227. [https://doi.org/10.1016/0009-2541\(76\)90036-X](https://doi.org/10.1016/0009-2541(76)90036-X)
- Rock N.M.S. 1991. *Lamprophyres*. New York, Blackie and Son, 285 p.
- Rogova V.P. 1966. Pseudoleucite rocks of the Murun alkali complex. *Doklady Academy of Sciences USSR. Earth Science Section*, **169**:170-173.
- Ruberti E., Enrich G.E.R., Azzone R.G., Comin-Chiaramonti P., De Min A., Gomes C.B. 2012. The Banhadão Alkaline Complex, southeastern Brazil: source and evolution of potassic SiO_2 -undersaturated high-Ca and low-Ca magmatic series. *Mineralogy and Petrology*, **104**:63-80. <https://doi.org/10.1007/s00710-011-0171-9>
- Sadowski G.R., Dias Neto C.M. 1981. O lineamento sismo-tectônico de Cabo Frio. *Revista Brasileira de Geociências*, **11**:209-212.
- Schorscher H.D., Shea M.E. 1992. The regional geology of the Poços de Caldas alkaline complex: mineralogy and geochemistry of selected nepheline syenites and phonolites. *Journal of Geochemical Exploration*, **45**:25-51. DOI: 10.1016/0375-6742(92)90121-N
- Shea M.E. 1992. Isotopic geochemical characteristics of selected nepheline syenites and phonolites from the Poços de Caldas alkaline complex. Minas Gerais, Brazil. *Journal of Geochemical Exploration*, **45**:173-214. DOI: 10.1016/0375-6742(92)90125-R
- Sonoki I.K., Garda G.M. 1988. Idades K-Ar de rochas alcalinas do Brasil meridional e Paraguai oriental: compilação e adaptação às novas constantes de decaimento. *Boletim IG-USP, Série Científica*, **19**:63-85.
- Sorensen H. 1974a. Alkali syenites, feldspathoidal syenites and related lavas. In: Sorensen H. (Ed.). *The Alkaline Rocks*. New York, Wiley, p. 22-52.
- Sorensen H. 1974b. Glossary of alkaline and related rocks. In: Sorensen H. (Ed.). *The Alkaline Rocks*. New York, Wiley, p. 577-588.
- Steiger R.H., Jäger E. 1977. Subcommittee on geochronology: Convention on the use of decay constants in geo- and cosmochemistry. *Earth and Planetary Science Letters*, **36**:359-362.
- Thompson R.N., Gibson S.A., Mitchell J.G., Dickin A.P., Leonardos O.H., Brod J.A., Greenwood J.C. 1998. Migrating Cretaceous-Eocene magmatism in the Serra do Mar alkaline province, SE Brazil: melts from the deflected Trindade mantle plume? *Journal of Petrology*, **39**:1493-1526.
- Ulbrich H.H.G.J. 1984. *A petrografia, a estrutura e o quimismo de nefelina sienitos do Maciço Alcalino de Poços de Caldas, MG-SP*. Thesis, Instituto de Geociências, Universidade de São Paulo, São Paulo, 480 p.
- Ulbrich H.H.G.J. 1986. As brechas de origem ígnea: Revisão e proposta para uma classificação geológica. *Boletim IG-USP Publicação Especial*, **3**. 78 p. <http://dx.doi.org/10.11606/issn.2317-8078.v0i3p01-82>
- Ulbrich H.H., Ulbrich M.N.C. 2000. The lujavrite and khibinite bodies in the Poços de Caldas alkaline massif, southeastern Brazil: a structural and petrographic study. *Revista Brasileira de Geociências*, **30**:615-622.
- Ulbrich H.H.G.J., Gomes C.B. 1981. Alkaline rocks from continental Brazil. *Earth Science Reviews*, **17**:135-154. [https://doi.org/10.1016/0012-8252\(81\)90009-X](https://doi.org/10.1016/0012-8252(81)90009-X)
- Ulbrich H.H.G.J., Vlach S.R.F., Demaiffe D., Ulbrich M.N.C. 2005. Structure and origin of the Poços de Caldas alkaline massif, SE Brazil. In: Comin-Chiaramonti P., Gomes C.B. (Eds.). *Mesozoic to Cenozoic Alkaline Magmatism in the Brazilian Platform*. São Paulo, EDUSP/FAPESP, p. 367-418.
- Ulbrich H.H.G.J., Vlach S.R.F., Ulbrich M.N.C., Kawashita K. 2002. Penecontemporaneous syenitic-phonolitic and basic-ultrabasic-carbonatitic rocks at the Poços de Caldas Alkaline Massif, SE Brazil. *Revista Brasileira de Geociências*, **32**:15-26.
- Ulbrich M.N.C. 1983. *Aspectos mineralógicos e petrológicos do Maciço Alcalino de Poços de Caldas, MG-SP*. Doctoral Thesis, Instituto de Geociências, Universidade de São Paulo, São Paulo, 369 p.
- Ulbrich M.N.C. 1993. Mineralogy of nepheline syenites from the Poços de Caldas alkaline massif, SE Brazil: chemistry, XR data and microtextures of feldspars. *Revista Brasileira de Geociências*, **23**:388-399.
- Vasconcelos P.M., Onoe A.T., Kawashita K., Soares A.J., Teixeira W. 2002. $^{40}\text{Ar}/^{39}\text{Ar}$ geochronology at the Instituto de Geociências, USP: instrumentation, analytical procedures, and calibration. *Anais da Academia Brasileira de Ciências*, **74**:297-342. <http://dx.doi.org/10.1590/S0001-37652002000200008>
- Vilalva F.C.J., Vlach S.R.F. 2004. Variações químicas em granada, espinélio e ilmenita de rochas lamprofíticas e sílico-carbonatíticas associadas ao Maciço Alcalino Poços de Caldas (MG-SP). In: Simpósio Internacional de Iniciação Científica, 12., São Paulo. *Anais...* Universidade de São Paulo, São Paulo. CD-ROM.
- Virgo D., Rosenhauer M., Huggins F.E. 1976. Intrinsic oxygen fugacities of natural melanites and schorlomite and crystal-chemical implications. *Annual Report of the Carnegie Institute of Washington* (1975-1976), p. 720-729.
- Vlach S.R.F., Ulbrich H.H.G.J., Ulbrich M.N.C. 1998. Isótopos radiogênicos (Sr, Nd) e estáveis (C, O) de rochas máfico-ultramáficas potássicas da região de Poços de Caldas, MG-SP: inferências sobre a natureza do manto litosférico mesozóico. In: Congresso Brasileiro de Geologia, 40., Belo Horizonte. *Anais...* p. 475.
- Vlach S.R.F., Ulbrich M.N.C., Ulbrich H.H.G.J., Gualda G.A.R. 1996. Rochas de afinidades alnoíticas e sílico-carbonatíticas periféricas ao Maciço Alcalino de Poços de Caldas (MG-SP). In: Congresso Brasileiro de Geologia, 39., Salvador. *Anais...* **2**:128-130.
- Vlach S.R.F., Vilalva F.C.J., Ulbrich M.N.C., Ulbrich H.H.G.J., Vasconcelos P.M. 2003. Phlogopite from carbonatitic veins associated with the Poços de Caldas Alkaline Massif, SE Brazil: mineralogy and $^{40}\text{Ar}/^{39}\text{Ar}$ dating by the laser step heating method. In: South American Symposium on Isotope Geology, 4., Salvador. *Short Papers...* p. 702-705.

